Black Phosphorus

International Edition: DOI: 10.1002/anie.201811181
German Edition: DOI: 10.1002/ange.201811181

Lattice Opening upon Bulk Reductive Covalent Functionalization of Black Phosphorus

Stefan Wild, Michael Fickert, Aleksandra Mitrovic, Vicent Lloret, Christian Neiss, José Alejandro Vidal-Moya, Miguel Ángel Rivero-Crespo, Antonio Leyva-Pérez, Katharina Werbach, Herwig Peterlik, Mathias Grabau, Haiko Wittkämper, Christian Papp, Hans-Peter Steinrück, Thomas Pichler, Andreas Görling, Frank Hauke, Gonzalo Abellán, and Andreas Hirsch**

Abstract: *The chemical bulk reductive covalent functionalization of thin-layer black phosphorus (BP) using BP intercalation compounds has been developed. Through effective reductive activation, covalent functionalization of the charged BP by reaction with organic alkyl halides is achieved. Functionalization was extensively demonstrated by means of several spectroscopic techniques and DFT calculations; the products showed higher functionalization degrees than those obtained by neutral routes.*

Since 2014, two-dimensional (2D) black phosphorus (BP) has attracted tremendous attention throughout the scientific community due to its high p-type charge carrier mobility and its tunable direct band gap.[1–9] In contrast to graphene, BP exhibits a marked puckering of the sp^3 structure, constituting a two-dimensional σ-only system, involving one lone electron pair at each P atom. Whereas its outstanding physical and materials properties have been intensively investigated, its chemistry remains almost unexplored.[10–12] Indeed, a first series of noncovalent functionalization protocols has been reported, mainly focused on improving the intrinsic instability of BP against water and oxygen.[13–17] Beyond these approaches, the covalent functionalization of the interface is one of the most promising routes for fine-tuning the chemical and physical properties of 2D nanomaterials.[18,19] In this sense, only a few recent reports on single-flake chemistry with diazonium salts,[20] and wet-chemistry on previously exfoliated flakes with nucleophiles[21–23] or carbon-free radicals[24] have been reported so far. This is probably due to the intrinsic low degree of reactivity of neutral BP towards these reactions and the difficulties associated with overcoming the huge van der Waals energy stored within a BP crystal, thus blocking the direct functionalization of BP. Along this front, a bulk wet-chemical derivatization sequence remains to be found. Moreover, an unambiguous determination of the covalent binding and its influence in the chemical structure of the P-layers is required to systematically explore the characteristics of BP reactivity.

To address these challenges we took advantage of the well-known reductive graphene chemistry using graphite intercalation compounds (GICs).[18,25–27] As a first success in this direction, we have recently reported the preparation of BP intercalation compounds (BPICs) with alkali metals (K and Na).[28] This paves the way for the exploration of the reductive route using activated negatively charged BP-*ite* nanosheets and electrophiles (E) as covalent reaction partners.

Herein, we provide the first real proof for covalent binding in BP with alkyl halides using a battery of characterization techniques. Furthermore, density functional theory (DFT) calculations were carried out to rationalize our results, providing a deep understanding of the covalent derivatization

[*] S. Wild, M. Fickert, Dr. A. Mitrovic, V. Lloret, Dr. F. Hauke, Dr. G. Abellán, Prof. A. Hirsch
Chair of Organic Chemistry II and Joint Institute of Advanced Materials and Processes (ZMP)
Friedrich-Alexander-Universität Erlangen-Nürnberg (FAU)
Nikolaus-Fiebiger Strasse 10, 91058 Erlangen and Dr.-Mack Strasse 81, 90762 Fürth (Germany)
E-mail: gonzalo.abellan@fau.de
andreas.hirsch@fau.de

Dr. C. Neiss, Prof. A. Görling
Lehrstuhl für Theoretische Chemie and Interdisciplinary Center of Molecular Materials (ICMM)
Friedrich-Alexander-Universität Erlangen-Nürnberg (FAU)
Egerlandstrasse 3, 91058 Erlangen (Germany)

Dr. J. A. Vidal-Moya, M. Á. Rivero-Crespo, Dr. A. Leyva-Pérez
Instituto de Tecnología Química
Universidad Politécnica de Valencia-Consejo Superior de Investigaciones Científicas
Avda. de los Naranjos s/n, 46022, Valencia (Spain)

K. Werbach, Prof. H. Peterlik, Prof. T. Pichler
Faculty of Physics, University of Vienna
Strudlhofgasse 4, 1090 Vienna (Austria)

M. Grabau, H. Wittkämper, Dr. C. Papp, Prof. Dr. H.-P. Steinrück
Lehrstuhl für Physikalische Chemie II, FAU
Egerlandstraße 3, 91058 Erlangen (Germany)

Dr. G. Abellán
Instituto de Ciencia Molecular (ICMol)
Universidad de Valencia
Catedrático José Beltrán 2, 46980, Paterna, Valencia (Spain)

Supporting information and the ORCID identification number(s) for the author(s) of this article can be found under: https://doi.org/10.1002/anie.201811181.

of BP. This thorough study reveals for the first time the lattice opening in BP, absent in graphene, which is a P-characteristic phenomenon in reduction chemistry, with the extreme case of K_3P formation with all P–P bonds cleaved.[28]

First, we investigated the in situ treatment of a potassium BPIC upon the addition of an electrophilic functionalization reagent (Scheme 1) followed by Raman spectroscopy.[28] In this experiment, we slowly evaporated hexyl iodide onto the previously synthesized BPIC KP_6, under ultrahigh-vacuum (UHV) conditions and measured constantly Raman spectra in order to monitor the course of the functionalization process in

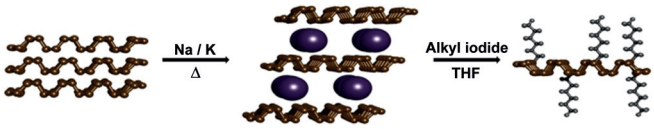

Scheme 1. General reaction course showing the reductive covalent functionalization of BP. Pristine BP is intercalated with an alkali metal in the solid state under controlled heating and afterwards the activated BPIC is dispersed in THF and reacted with an electrophilic trapping reagent.

situ. The BP was previously intercalated in a glovebox under Argon atmosphere and transferred into the UHV reaction chamber (SI 1). As depicted in Figure 1 a), highlighted in gray, a series of new distinct Raman modes arise below 400 cm^{-1} concomitantly with increasing amounts of the reacted electrophilic hexyl iodide. More specifically, a sharp peak at 145 cm^{-1}, a broad shoulder around 210 cm^{-1}, two broad features between 270 and 320 cm^{-1}, and a small peak between the A_g^1 and B_{2g} peak at 405 cm^{-1} can be clearly observed, strongly suggesting modification of the 2D BP lattice with the formation of a P–C bond.

We carried out DFT calculations simulating the covalent attachment of a methyl group to BP and calculating the expected Raman spectra. We used a 4×3 super cell of BP, with one methyl group added. We considered several binding scenarios, including the formation of positively charged phosphonium salts, the influence of K and I, the functionalization degree, and the monotopic/antaratopic functionalization. Interestingly, the resulting structures, after a full geometry relaxation was allowed, repeatedly exhibit one localized unpaired electron as well as an elongated P–P bond next to the P–C bond, specifically from 2.26 to 2.83 Å, leading to a lattice opening (Scheme 2, Figure SI 2). As this resulting radical species is expected to be highly reactive, we also considered saturation by iodine or potassium, which would remove spin polarization (radical character) of the methylated BP single layer (Figure SI 3). Figure 1 b shows the calculated Raman spectra for a methylated BP single layer in the presence of potassium (further calculations can be found in Figures SI 4–6), which takes into account that the vapor–solid reaction was not quenched in the in situ experiment, and therefore the potassium definitely remains in the resulting compound. According to our calculations the intensities—especially of the low-frequency bands—are quite sensitive to the degree of functionalization, charge, and presence of

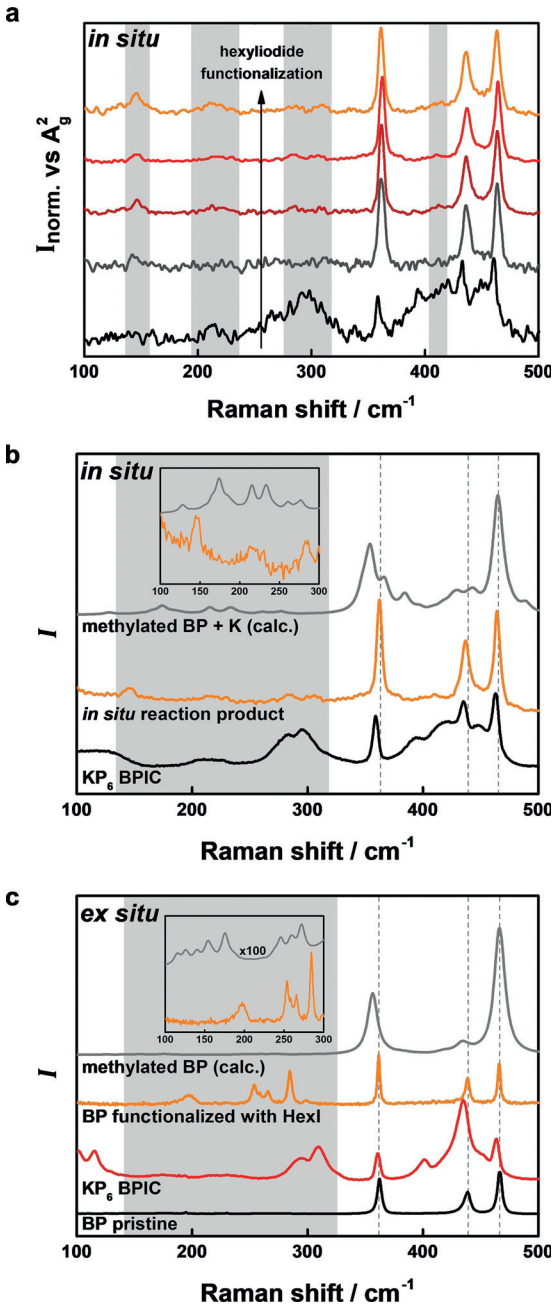

Figure 1. a) In situ Raman spectroscopy monitoring the reaction of hexyl iodide with KP_6 using an excitation wavelength of $\lambda_{exc}=633$ nm. With increasing amounts of hexyl iodide distinct new Raman peaks arise at 145, 210, between 260 and 285, and at 410 cm^{-1}. b) Calculated Raman spectrum of a methylated BP single layer saturated with potassium. The inset shows a magnification of the region below 300 cm^{-1} for better comparison. The calculated spectrum has been shifted by 15 cm^{-1}. c) Mean Raman spectra visualizing the reaction course of the covalent functionalization of BP ex situ. The calculated Raman spectrum of a BP single layer with one added methyl group is also included. The inset magnifies the region below 300 cm^{-1} for better comparison. The calculated spectrum has been shifted by 14 cm^{-1}.

counter ions (see Figures SI 10, SI 4–6). In this sense, the predicted Raman spectrum of a methylated BP monolayer saturated with potassium is in good agreement with our

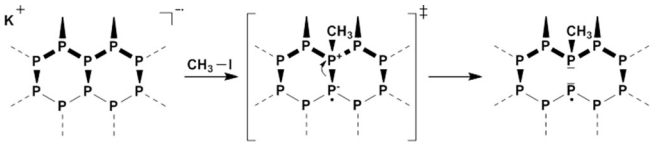

Scheme 2. Lattice opening of BP upon covalent modification with methyl iodide: proposed reaction mechanism based on DFT calculations.

experimental results (to correct for systematically too low frequencies, the calculated spectra were shifted to match the experimental A_g^2 band at 467 cm^{-1}).

Moreover, we obtain the same results when using Na BPICs instead of K BPICs (Figure SI 7). This is in clear contrast with GICs chemistry, in which the Na-intercalation compounds cannot be achieved without using $Na^+(G_x)_y$ complexes, where G accounts for linear ethylene glycol dimethyl ether homologues ("glymes").[29]

In the next step, we focused on the bulk reductive functionalization of BP using the wet-chemical approach.[18,30] For this, pristine BP was intercalated with sodium or potassium to yield the respective BPIC (NaP_6 or KP_6), which was then dispersed in purified tetrahydrofuran (THF) by applying ultrasonication, and finally quenched with alkyl halides (Scheme 1). After filtration in the glovebox, the reaction product was obtained in the form of a dark gray powder. Statistical Raman spectroscopy (SRS) using an excitation wavelength of 633 nm revealed the appearance of a new band at around 145 cm^{-1}, which was also observed in the in situ experiment, and new Raman modes in the 250–300 cm^{-1} region (see Figure 1 c). Our calculations of methylated BP layers reproduce Raman bands below 300 cm^{-1}. These intensities and positions critically depend both on the degree of functionalization and presence of counter ions, however. As an example, the calculated Raman spectrum of a methylated BP monolayer is shown in Figure 1 c.

One could have expected that the electrophilic trapping with hexyl iodide would lead to the formation of 2D BP phosphonium sites incorporated in an otherwise intact hexagonal P-lattice, with a formal positive charge in the alkylated P atoms. However, our DFT calculations points towards a P–P bond cleavage (Scheme 2), and we only obtain a phosphonium if a whole positive charge is included on the BP sheet. In this scenario we find a Raman fingerprint at 315 cm^{-1} (Figure SI 6), which is absent in the experimental data. To further check the suitability of the calculations, we also developed the functionalization reaction with methyl iodide, which showed a rather good agreement with the predictions (Figures SI 5 and 8). According to our calculations, we assume that the occurrence of these distinct peaks is related to P–P vibrations originating from lattice distortions in the BP sheet (see Supporting Information Videos).

Moreover, the peaks at around 195 and 230 cm^{-1} can be associated with turbostratic disordering of individual layers or edge phonons in the BP lattice and can even be measured in pristine BP.[31,13] We have checked the suitability of the reaction using both Na BPICs and K BPICs, and methyl and hexyl iodide. Mean Raman spectra (> 50 single point spectra) repeatedly exhibit the same behavior with clear bands at ca. 145, 217, and 308 cm^{-1}, thus confirming the successful functionalization reaction and the homogeneity of the samples (Figures SI 8 and 11). The influence of the excitation wavelength (533 and 633 nm) shows minor changes in the relative intensity of the new modes (Figure SI 9). The crystallinity of the methyl-functionalized specimen was also investigated via X-ray diffraction (for experimental details see Figure SI 12). The results can be described by a model with a few separated planes, where the symmetry along the *b*-axis—the crystal structure of BP is made up of puckered layers of atoms stacked along the crystallographic *b*-axis—has been lost, thus confirming the results obtained by Raman spectroscopy.

In order to gain more information about the chemical composition of the covalently attached addends, thermogravimetric analysis coupled to mass spectrometry (TG-MS) measurements were conducted. Figure 2 a and Figure SI 13 depict the mass loss of the covalently modified BP sample upon heating up to 600 °C, which contains three interesting features. First, two mass losses between 100 °C and 300 °C can be attributed to the detachment of the hexyl chain from the BP lattice ($m/z = 85$ and its typically related mass fragments $m/z = 56$ and $m/z = 41$). The differences in the temperatures may be related to different binding sites: basal plane atoms (zigzag and armchair), positions near the edges, or on the rims[32] Secondly, the sharp mass loss of the sample above 400 °C can be explained by the complete decomposition of BP to P_4 and P_4-based clusters ($m/z = 31$, 62, 93, and 124). Indeed, compared to pristine BP prepared under the same conditions but without functionalization reaction, the degradation tem-

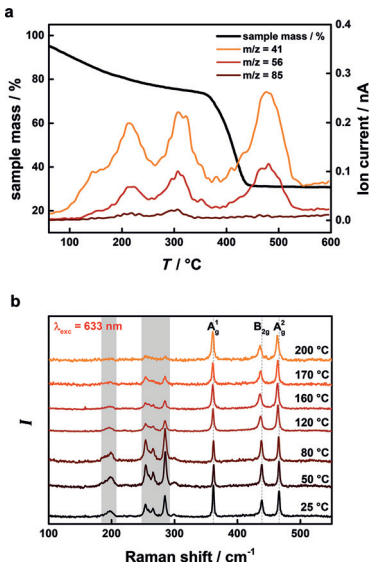

Figure 2. a) TG-MS displays a significant mass loss below 200 °C which can be correlated to the detachment of the covalently bound hexyl groups before the BP lattice decomposes to P_4 above 400 °C. The MS data shows characteristic mass fragments of the hexyl groups at $m/z = 85$, 56, and 41. b) Temperature-dependent Raman spectroscopy. The disappearance of the Raman modes below 300 cm^{-1} at temperatures above 170 °C can be attributed to the defunctionalization of BP, demonstrating the reversibility of the reaction.

perature shifts from ca. 330 to 360 °C, highlighting the increase of the thermal stability (Figure SI 14). Moreover, neither hexyl iodide ($m/z = 212$), I_2 ($m/z = 254$), nor its monoatomic equivalent ($m/z = 127$) were detected (Figure SI 13). This observation points towards the formation of the side product KI between the leaving group iodide and the K, which has a melting point of 723 °C and thus cannot be detected in the measurement. As a matter of fact, the residual mass loss in the functionalized sample is ca. 30 %, which could be related to the presence of KI due to its poor solubility in THF during the workup (vide infra), as well as the thermal formation of graphitic carbon from the addends (Figure SI 15). These assumptions can be confirmed by the solubilization of KI in an aqueous solution of silver nitrate as well as the presence of benzene mass fragments, typically associated with nanocarbon degradation.[30] Finally, the abrupt mass loss at around 480 °C may be related to trapped alkyl moieties between the layers, the formation of P-based nanoforms like nanoribbons, or cluster-like species.

In order to demonstrate the covalent binding of the alkyl chains and investigate the reversibility of the functionalization reaction, we performed a temperature-dependent SRS analysis. We conducted Raman mappings of the functionalized flakes deposited on Si/SiO_2 wafers increasing the temperature from 20 up to 220 °C (Figure 2b and Figure SI 16). The three main modes of BP can be clearly seen as well as the characteristic peaks below 300 cm^{-1} related to the covalent functionalization, which are highlighted in gray. Upon heating, the intensity of these modes starts to decrease at temperatures above 160 °C, until they nearly vanish at 200 °C in agreement with the TG-MS analysis, indicating the defunctionalization of the BP lattice. Here, it should be mentioned that also the A_g^1, B_{2g}, and A_g^2 modes decrease in absolute intensity with increasing temperature, which is explained by the thermal instability of FL-BP.[14]

Compared to other recent reports about the neutral covalent functionalization of BP using diazonium salts[20] or nucleophilic molecules,[21] in which no significant change in the Raman fingerprint was observed, our results indicate a higher degree of functionalization. We also carried out the functionalization of BP with hexyl iodide without alkali metal intercalation using exactly the same experimental settings. Note that for the neutral route, a previous step of liquid-phase exfoliation is required prior to the functionalization. Additionally, we explored different reaction temperatures and solvents (THF and NMP (*N*-Methyl-2-pyrrolidone)), as well as inert and ambient conditions (see Figure SI 17). Related Raman spectra show no additional vibrational modes besides the B_{3g} and B_{1g} modes already mentioned at 194 and 230 cm^{-1}. Also, in TG-MS analysis, no mass loss around 200 °C and no characteristic mass fragments were detected (Figure SI 18).

Investigations with X-ray diffraction were performed in analogy to the experiments with methyl-functionalized BP. Functionalized with hexyl iodide, BP exhibits a higher order and probably features a few-layer phase (as observed in methylated BP) and a compressed phase with three-dimensional order (see Figure SI 12). We also conducted XPS measurements, obtaining direct proof for the formation of a P–C bond. In Figure 3 (see Figure SI 19 for the related survey spectrum), the P 2p region of pristine BP and of the covalently modified analogue is shown. The fit comprises three spin-orbit split doublets (splitting of 0.78 eV) assigned to pristine BP P^0 (black), oxidized phosphorus $P^{P\text{-}O}$ (red), and carbon-bound phosphorus $P^{P\text{-}C}$ (orange). The P $2p_{3/2}$ signal of the P^0 species was set at 130.1 eV, which is the value determined from the measurement of the pristine BP sample, and is in agreement with a value of 130.06 eV reported for crystalline BP.[8] For the analysis of the samples, the chemical shift between pristine and oxidized phosphorous is constrained to be 4.1 eV, in accordance to the pristine sample. The analysis shows that for the hexyl-functionalized sample a carbon-bound species with a chemical shift of +2.7 eV relative to the P^0 signal is observed. This gives further experimental support for the successful covalent modification of the BP lattice.

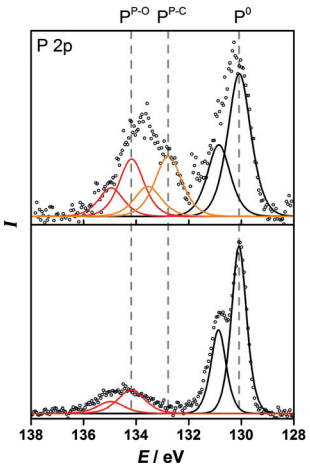

Figure 3. XP spectrum of covalently functionalized BP with hexyl iodide (top) compared to that of pristine BP (bottom). The P 2p region is shown, with the $2p_{1/2}$ and $2p_{3/2}$ components of the doublets separated by 0.78 eV; the positions of the $2p_{3/2}$ levels are indicated by vertical dashed lines. The fits for the P^0, $P^{P\text{-}C}$, and the oxidized $P^{P\text{-}O}$ species are shown by black, orange, and red lines, respectively.

Concerning stability, we have evaluated the final functionalized flakes upon exposure to oxygen and moisture by measuring the scanning Raman microscopy (SRM) immediately after functionalization and after 15 days, showing the typical exponential decay of the Raman modes, and reflecting its degradation (Figure SI 20). Furthermore, we have evaluated with XPS the influence of water on the covalent functionalization procedure. For this, we have submitted the sample to a final aqueous washing step during the workup process. Interestingly, the spin-orbit split doublets assigned to the formation of P–C bonds dramatically decrease (Figure SI 21), while the peaks associated with potassium and iodine almost completely disappeared (data not shown), due to the high solubility of the corresponding ions in water. These results point towards a water-assisted defunctionalization of the BP lattice.

Finally, to gain unambiguous evidence for the covalent bond formation we conducted quantitative magic-angle-spinning ^{31}P solid-state NMR (^{31}P MAS NMR) experiments. Figure 4A depicts the spectra of intercalated KP_6, clearly

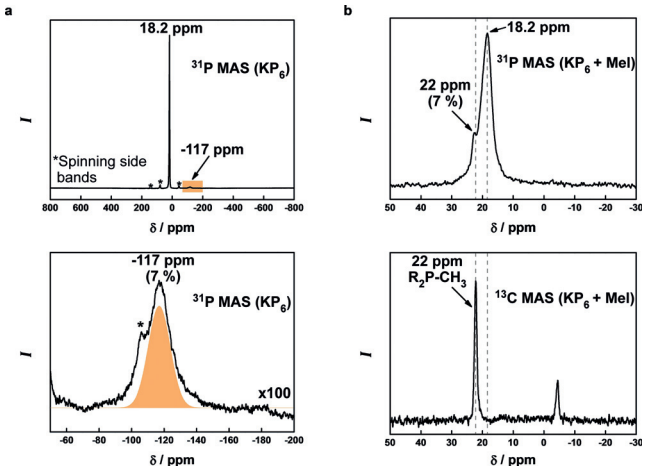

Figure 4. a) ^{31}P MAS NMR spectra of intercalated BP (KP_6) featuring the signal for pristine black phosphorus at 18.2 ppm as well as a signal at −117 ppm, which can be assigned to axially coordinated P atoms bearing a localized negative charge. b) Top: ^{31}P MAS NMR spectrum of BP functionalized with methyl moieties showing the appearance of a new signal at 22 ppm confirming the presence of P–CH_3 species. Bottom: Accordingly, the ^{13}C MAS NMR spectrum acquired in ^{1}H–^{31}P cross-polarization mode shows the disappearance of the original BP signal at 18.2 ppm and the persistence of the signal at 22 ppm; this strongly supports the formation of a covalent P–CH_3 bond.

showing the expected signal for phosphorene at 18.2 ppm plus a single new signal at −117 ppm, which can be assigned to axially coordinated P atoms bearing a localized negative charge; this corresponds to ≈7% of the total P atoms.[33] These upfield-shifted P atoms nicely agree with the theoretically proposed P atoms pop out of the 2D framework after receiving electronic density from K in the BPIC structure (Figure SI 3). Along these lines, the ^{31}P MAS NMR spectrum of the methylated BP shows the complete disappearance of the negatively charged P atoms, and the appearance of a new signal at 22 ppm, a value that very precisely matches that expected for a P–CH_3 and not for a P^+–CH_3 bond; this signal integrates for ≈7% of the total P atoms after deconvolution (Figure 4B). Moreover, ^{13}C MAS NMR results also support the formation of new P–CH_3 bonds (and not the corresponding phosphonium species). In order to further confirm the functionalization, the MAS-NMR spectrum was acquired in ^{1}H–^{31}P cross-polarization mode, such that only the P atoms bearing H atoms at a distance of one or two bonds are detected (Figure 4B). The corresponding spectra shows the persistence of the signal at 22 ppm and the complete disappearance of the original phosphorene signal at 18.2 ppm, which strongly supports the formation of a covalent P–CH_3 bond.

Together, these NMR results indicate that in KP_6 BPIC ≈7% of the localized and negatively charged P atoms react quantitatively in a substitution reaction with methyl iodide to give new covalent P–CH_3 bonds and KI, in stark contrast to the neutral route (Figure SI 22). This reductive route for the covalent modification of BP results in a better degree of functionalization than that of related alkyl-functionalized graphene and, in terms of solubility, similar behavior in *ortho*-dichlorobenzene (*o*-DCB), indicative of improved processability (Figure SI 23).[30]

In conclusion, the reductive covalent functionalization of BP with alkyl halides using intercalation compounds results in a remarkably high degree of functionalization and involves a P–P bond breakage (Scheme 2). These results open new pathways for fine-tuning the chemical and physical properties of BP, as well as developing unprecedented hybrid materials.

Acknowledgements

A.H. and G.A. acknowledge the European Research Council (ERC Advanced Grant 742145 B-PhosphoChem to A.H., and ERC Starting Grant 2D-PnictoChem 804110 to G.A.) for support. The research leading to these results was partially funded by the European Union Seventh Framework Programme under grant agreement No. 604391 Graphene Flagship. G.A. has received financial support through the Postdoctoral Junior Leader Fellowship Programme from "la Caixa" Banking Foundation (LCF/BQ/PI18/11630018). G.A. thanks the Deutsche Forschungsgemeinschaft (DFG; FLAG-ERA AB694/2-1), the Generalitat Valenciana (SEJI/2018/034 grant), and the FAU (Emerging Talents Initiative grant #WS16-17_Nat_04) for support. A.H. and A.G. thank the SFB 953 "Synthetic Carbon Allotropes" funded by the DFG for support and the Cluster of Excellence "Engineering of Advanced Materials". A.G. is grateful for funding from the Free State of Bavaria (Research Network "Solar Technologies go Hybrid"). A.M. thanks the Alexander von Humboldt (AvH) Foundation for a postdoctoral fellowship. This work was supported by the MINECO (Spain) through the Excellence Unit María de Maeztu (MDM-2015-0538) and the Project CTQ2017-86735-P.

Conflict of interest

The authors declare no conflict of interest.

Keywords: ^{31}P NMR spectroscopy · black phosphorus · covalent functionalization · Raman spectroscopy · reductive route

How to cite: *Angew. Chem. Int. Ed.* **2019**, *58*, 5763–5768
Angew. Chem. **2019**, *131*, 5820–5826

[1] J. D. Wood, S. A. Wells, D. Jariwala, K.-S. Chen, E. Cho, V. K. Sangwan, X. Liu, L. J. Lauhon, T. J. Marks, M. C. Hersam, *Nano Lett.* **2014**, *14*, 6964–6970.
[2] A. Castellanos-Gomez, L. Vicarelli, E. Prada, J. O. Island, K. L. Narasimha-Acharya, S. I. Blanter, D. J. Groenendijk, M. Buscema, G. A. Steele, J. V. Alvarez, et al., *2D Mater.* **2014**, *1*, 025001.
[3] M. Buscema, D. J. Groenendijk, G. A. Steele, H. S. J. van der Zant, A. Castellanos-Gomez, *Nat. Commun.* **2014**, *5*, 4651.
[4] J. Qiao, X. Kong, Z.-X. Hu, F. Yang, W. Ji, *Nat. Commun.* **2014**, *5*, 4475.
[5] F. Xia, H. Wang, Y. Jia, *Nat. Commun.* **2014**, *5*, 4458.
[6] L. Li, Y. Yu, G. J. Ye, Q. Ge, X. Ou, H. Wu, D. Feng, X. H. Chen, Y. Zhang, *Nat. Nanotechnol.* **2014**, *9*, 372–377.

[7] L. Li, F. Yang, G. J. Ye, Z. Zhang, Z. Zhu, W. Lou, X. Zhou, L. Li, K. Watanabe, T. Taniguchi, et al., *Nat. Nanotechnol.* **2016**, *11*, 593 – 597.
[8] L. Li, J. Kim, C. Jin, G. J. Ye, D. Y. Qiu, F. H. da Jornada, Z. Shi, L. Chen, Z. Zhang, F. Yang, et al., *Nat. Nanotechnol.* **2017**, *12*, 21 – 25.
[9] B. G. Márkus, F. Simon, K. Nagy, T. Fehér, S. Wild, G. Abellán, J. C. Chacón-Torres, A. Hirsch, F. Hauke, *Phys. Status Solidi B* **2017**, *254*, 1700232.
[10] A. Favron, E. Gaufrès, F. Fossard, A.-L. Phaneuf-L'Heureux, N. Y.-W. Tang, P. L. Lévesque, A. Loiseau, R. Leonelli, S. Francoeur, R. Martel, *Nat. Mater.* **2015**, *14*, 826 – 832.
[11] A. Hirsch, F. Hauke, *Angew. Chem. Int. Ed.* **2018**, *57*, 4338 – 4354; *Angew. Chem.* **2018**, *130*, 4421 – 4437.
[12] R. Gusmão, Z. Sofer, M. Pumera, *Angew. Chem. Int. Ed.* **2017**, *56*, 8052 – 8072; *Angew. Chem.* **2017**, *129*, 8164 – 8185.
[13] G. Abellán, S. Wild, V. Lloret, N. Scheuschner, R. Gillen, U. Mundloch, J. Maultzsch, M. Varela, F. Hauke, A. Hirsch, *J. Am. Chem. Soc.* **2017**, *139*, 10432 – 10440.
[14] G. Abellán, V. Lloret, U. Mundloch, M. Marcia, C. Neiss, A. Görling, M. Varela, F. Hauke, A. Hirsch, *Angew. Chem. Int. Ed.* **2016**, *55*, 14557 – 14562; *Angew. Chem.* **2016**, *128*, 14777 – 14782.
[15] Y. Zhao, Q. Zhou, Q. Li, X. Yao, J. Wang, *Adv. Mater.* **2017**, *29*, 1603990.
[16] V. V. Korolkov, I. G. Timokhin, R. Haubrichs, E. F. Smith, L. Yang, S. Yang, N. R. Champness, M. Schröder, P. H. Beton, *Nat. Commun.* **2017**, *8*, 1385.
[17] S. Walia, S. Balendhran, T. Ahmed, M. Singh, C. El-Badawi, M. D. Brennan, P. Weerathunge, M. N. Karim, F. Rahman, A. Rassell, et al., *Adv. Mater.* **2017**, *29*, 1700152.
[18] J. M. Englert, C. Dotzer, G. Yang, M. Schmid, C. Papp, J. M. Gottfried, H.-P. Steinrück, E. Spiecker, F. Hauke, A. Hirsch, *Nat. Chem.* **2011**, *3*, 279 – 286.
[19] D. Voiry, A. Goswami, R. Kappera, C. de C. C. e. Silva, D. Kaplan, T. Fujita, M. Chen, T. Asefa, M. Chhowalla, *Nat. Chem.* **2015**, *7*, 45 – 49.
[20] C. R. Ryder, J. D. Wood, S. A. Wells, Y. Yang, D. Jariwala, T. J. Marks, G. C. Schatz, M. C. Hersam, *Nat. Chem.* **2016**, *8*, 597 – 602.
[21] Z. Sofer, J. Luxa, D. Bouša, D. Sedmidubský, P. Lazar, T. Hartman, H. Hardtdegen, M. Pumera, *Angew. Chem. Int. Ed.* **2017**, *56*, 9891 – 9896; *Angew. Chem.* **2017**, *129*, 10023 – 10028.
[22] Y. Cao, X. Tian, J. Gu, B. Liu, B. Zhang, S. Song, F. Fan, Y. Chen, *Angew. Chem. Int. Ed.* **2018**, *57*, 4543 – 4548; *Angew. Chem.* **2018**, *130*, 4633 – 4638.
[23] M. van Druenen, F. Davitt, T. Collins, C. Glynn, C. O'Dwyer, J. D. Holmes, G. Collins, *Chem. Mater.* **2018**, *30*, 4667 – 4674.
[24] H. Hu, H. Gao, L. Gao, F. Li, N. Xu, X. Long, Y. Hu, J. Jin, J. Ma, *Nanoscale* **2018**, *10*, 5834 – 5839.
[25] S. Chakraborty, J. Chattopadhyay, W. Guo, W. E. Billups, *Angew. Chem. Int. Ed.* **2007**, *46*, 4486 – 4488; *Angew. Chem.* **2007**, *119*, 4570 – 4572.
[26] P. Vecera, J. Holzwarth, K. F. Edelthalhammer, U. Mundloch, H. Peterlik, F. Hauke, A. Hirsch, *Nat. Commun.* **2016**, *7*, 12411.
[27] P. Vecera, J. C. Chacón-Torres, T. Pichler, S. Reich, H. R. Soni, A. Görling, K. Edelthalhammer, H. Peterlik, F. Hauke, A. Hirsch, *Nat. Commun.* **2017**, *8*, 15192.
[28] G. Abellán, C. Neiss, V. Lloret, S. Wild, J. C. Chacón-Torres, K. Werbach, F. Fedi, H. Shiozawa, A. Görling, H. Peterlik, et al., *Angew. Chem. Int. Ed.* **2017**, *56*, 15267 – 15273; *Angew. Chem.* **2017**, *129*, 15469 – 15475.
[29] L. Seidl, N. Bucher, E. Chu, S. Hartung, S. Martens, O. Schneider, U. Stimming, *Energy Environ. Sci.* **2017**, *10*, 1631 – 1642.
[30] G. Abellán, M. Schirowski, K. F. Edelthalhammer, M. Fickert, K. Werbach, H. Peterlik, F. Hauke, A. Hirsch, *J. Am. Chem. Soc.* **2017**, *139*, 5175 – 5182.
[31] H. B. Ribeiro, C. E. P. Villegas, D. A. Bahamon, D. Muraca, A. H. C. Neto, E. A. T. de Souza, A. R. Rocha, M. A. Pimenta, C. J. S. de Matos, *Nat. Commun.* **2016**, *7*, 12191.
[32] X.-P. Kong, X. Shen, J. Jang, X. Gao, *J. Phys. Chem. Lett.* **2018**, *9*, 947 – 953.
[33] O. Kühl, *Phosphorus-31 NMR Spectroscopy: A Concise Introduction for the Synthetic Organic and Organometallic Chemist*, Springer Science & Business Media, Berlin, **2008**.

Manuscript received: September 28, 2018
Revised manuscript received: January 18, 2019
Accepted manuscript online: January 24, 2019
Version of record online: March 21, 2019

